JOURNAL OF VIROLOGY, Aug. 2007, p. 8552–8562 Vol. 81, No. 16
0022-538X/07/$08.00+0 doi:10.1128/JVI.00924-07
Copyright © 2007, American Society for Microbiology. All Rights Reserved.

Caveolar Endocytosis Is Critical for BK Virus Infection of Human Renal Proximal Tubular Epithelial Cells▽

Takahito Moriyama,[1] J. Pablo Marquez,[2] Tetsuro Wakatsuki,[2] and Andrey Sorokin[1]*

Division of Nephrology and Kidney Disease Center, Department of Medicine,[1] and Biotechnology and Bioengineering Center, Department of Physiology,[2] Medical College of Wisconsin, Milwaukee, Wisconsin 53226

Received 30 April 2007/Accepted 24 May 2007

In recent years, BK virus (BKV) nephritis after renal transplantation has become a severe problem. The exact mechanisms of BKV cell entry and subsequent intracellular trafficking remain unknown. Since human renal proximal tubular epithelial cells (HRPTEC) represent a main natural target of BKV nephritis, analysis of BKV infection of HRPTEC is necessary to obtain additional insights into BKV biology and to develop novel strategies for the treatment of BKV nephritis. We coincubated HRPTEC with BKV and the cholesterol-depleting agents methyl beta cyclodextrin (MBCD) and nystatin (Nys), drugs inhibiting caveolar endocytosis. The percentage of infected cells (detected by immunofluorescence) and the cellular levels of BKV large T antigen expression (detected by Western blot analysis) were significantly decreased in both MBCD- and Nys-treated HPRTEC compared to the level in HRPTEC incubated with BKV alone. HRPTEC infection by BKV was also tested after small interfering RNA (siRNA)-dependent depletion of either the caveolar structural protein caveolin-1 (Cav-1) or clathrin, the major structural protein of clathrin-coated pits. BKV infection was inhibited in HRPTEC transfected with Cav-1 siRNA but not in HRPTEC transfected with clathrin siRNA. The colocalization of labeled BKV particles with either Cav-1 or clathrin was investigated by using fluorescent microscopy and image cross-correlation spectroscopy. The rate of colocalization of BKV with Cav-1 peaked at 4 h after incubation. Colocalization with clathrin was insignificant at all time points. These results suggest that BKV entered into HRPTEC via caveolae, not clathrin-coated pits, and that BKV is maximally associated with caveolae at 4 h after infection, prior to relocation to a different intracellular compartment.

BK virus (BKV), one of 14 polyomaviruses, is a nonenveloped double-stranded DNA virus with a 40- to 44-nm-sized icosahedral capsid. This capsid contains a 5,000-base-pair genome that encodes three capsid proteins, viral proteins 1, 2, and 3 (VP1, -2, and -3), and two nonstructural polypeptides, large tumor antigen (T-Ag) and small tumor antigen. Other well-studied polyomaviruses are JC virus (JCV), murine polyomavirus (mPy), and simian virus 40 (SV40). Only BKV and JCV are known to infect humans.

BKV was initially isolated from the urine of renal transplant patients with ureteral stenosis in 1971 (14). BKV infection became a major issue for renal transplant patients only in recent years, because of more efficient immunosuppressive therapies, such as tacrolimus, cyclosporine A, and mycophenolate mofetil, for renal transplant patients. Primary BKV infection occurs until age 10 without obvious symptoms. More than 80% of the population is infected by BKV, and approximately 50% of healthy native kidneys contain latent BKV (27). Although potent immunosuppressive therapies are useful for acute and chronic rejection, they become a risk factor for the progression of latent BKV to BKV nephritis. A prevalence of BKV nephritis in renal transplant patients of 5 to 10% has been reported. Progressive renal failure which induces graft loss has been estimated as occurring in approximately 40 to 60% of these cases. At present, no specific agent against BKV nephritis is available. Actually, the only efficient therapy against BKV nephritis appears to be a reduction/change of immunosuppressive agents, though it may increase the inherent risk of rejection (13, 18–22, 37, 38). The typical renal histological finding of BKV nephritis is tubulointerstitial change, with scattered interstitial inflammatory cell infiltration, lysis, atrophy, and necrosis of the tubular epithelium, as well as expansion and fibrosis of the interstitium (7). A few glomerular changes were also reported, with the most-frequent viral cytopathic effect seen in the Bowman's capsular epithelium (3). Considering these facts, human renal proximal epithelial cells (HRPTEC) are considered to be one of the main natural targets of BKV.

Though it was reported that BKV is capable of infecting HRPTEC in vitro (24), little is known about the exact mechanisms of BKV entry into HRPTEC and its subsequent intracellular trafficking to the nucleus in vitro. BKV was reported to enter into monkey-derived Vero cells through a caveola-mediated pathway, and internalization depended upon an intact microtubule network (11, 12). As revealed by electron microscopy, HRPTEC contains all the ultrastructural features required for caveola-mediated internalization (8). Caveolae (caveolin-containing lipid rafts) are flask-shaped plasma membrane invaginations with a diameter of 50 to 80 nm, enriched in cholesterol and sphingolipids. They are found in most cells, including HRPTEC. Even though caveolae participate in multiple processes, including the transcytosis of macromolecules, regulation of transduction of various signaling molecules, and transportation of cholesterol from intracellular organelles to

* Corresponding author. Mailing address: Division of Nephrology and Kidney Disease Center, Department of Medicine, Medical College of Wisconsin, 8701 Watertown Plank Road, Milwaukee, WI 53226. Phone: (414) 456-4438. Fax: (414) 456-6515. E-mail: sorokin@mcw.edu.

▽ Published ahead of print on 6 June 2007.

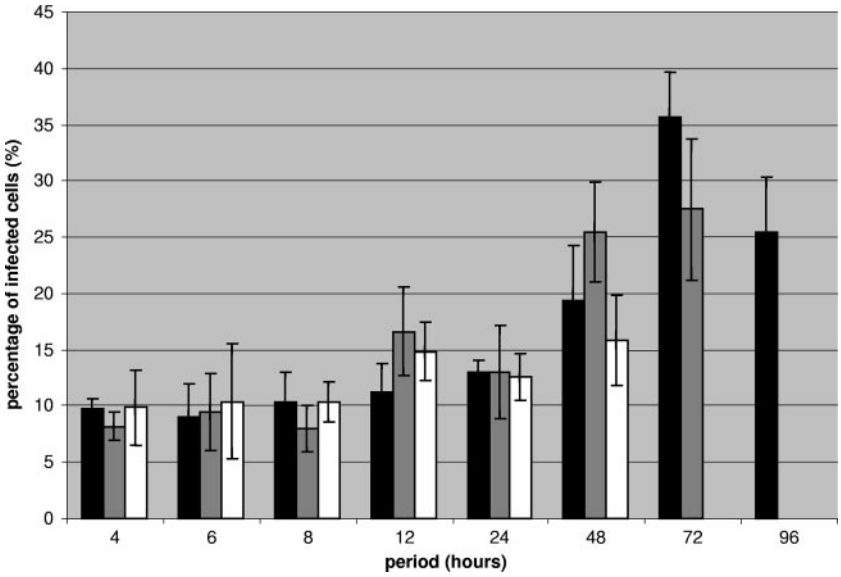

FIG. 1. Percentages of BKV-infected cells. HRPTEC were incubated with several doses of BKV (MOI, 0.5 to 5 FFU/cell) for different periods of time (4 to 96 h). At 48 h after this incubation period, the cells were fixed and analyzed by IF. The percentage of infected cells was calculated by the formula T-Ag-positive cells/total cells × 100. At least 500 cells were counted in each coverslip, and the means and SE were calculated from the results for three different coverslips. We could not show the result for the MOI of 0.5 FFU/cell at 96 h and the results for the MOI of 0.75 FFU/cell at the 72- and 96-h incubation periods because infected cells consistently detached from the coverslips.

extracellular acceptors, their specific functions depend on their host cells (6, 34, 36).

In this report, we examined BKV entry into HRPTEC through caveolae by using methyl beta cyclodextrin (MBCD) and nystatin (Nys) as cholesterol-depleting agents. We also examined the role of caveolin-1 (Cav-1), which is a main component of caveolae and acts as a scaffolding protein, by transfection with the small interfering RNAs (siRNA) of Cav-1 and clathrin, which is a major structural protein of clathrin-coated pits, as the control. We examined the colocalization of cesium

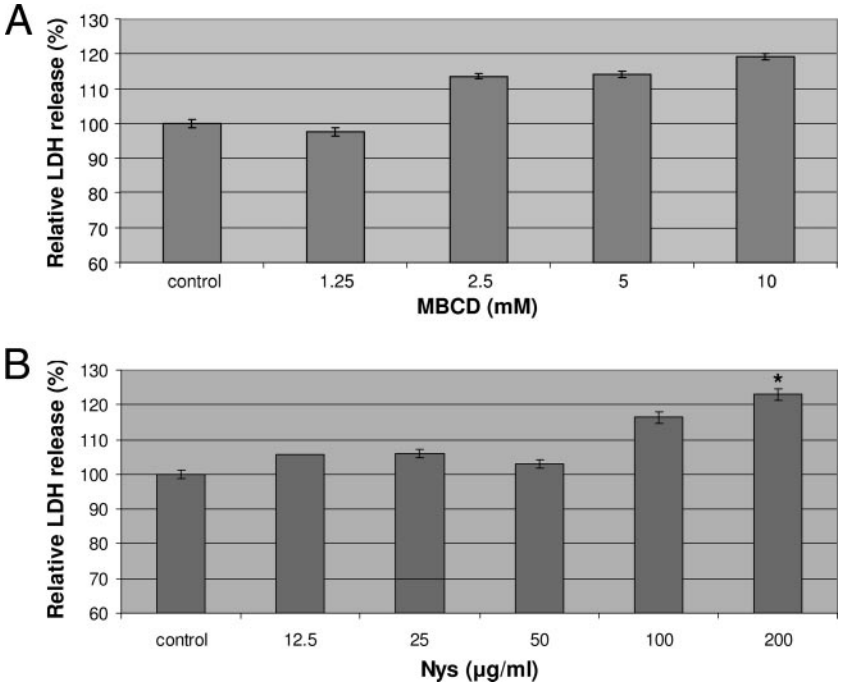

FIG. 2. Cytotoxicity assays of MBCD (A) and Nys (B). HRPTEC were incubated with MBCD (1.25, 2.5, 5, and 10 mM) and Nys (12.5, 25, 50, 100, and 200 μg/ml) for 5 days. Control, HRPTEC were not incubated with either MBCD or Nys. After incubation, supernatants and cell lysate were used for measuring the levels of LDH released. LDH was measured from five different wells for each dose. Means and SE were calculated from the results for 10 different wells from two independent examinations. *, $P < 0.05$.

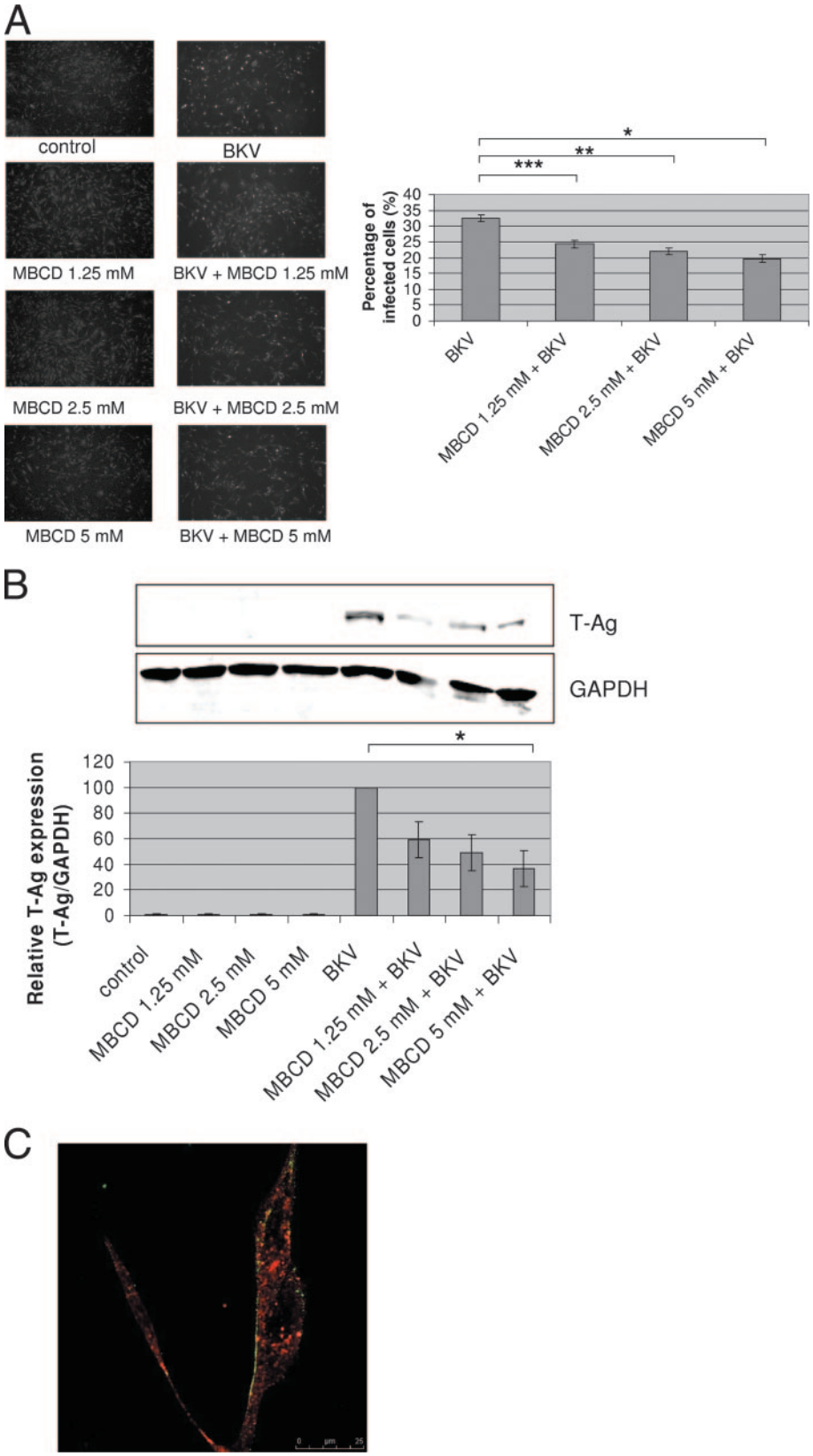

FIG. 3. MBCD interfered with BKV infection. HRPTEC were preincubated with MBCD (1.25, 2.5, and 5 mM) for 1 h prior to coincubation with BKV (MOI, 0.5 FFU/cell). After 72 h, medium was removed and cells were washed three times with REBM with 0.5% FBS and incubated for another 48 h with fresh medium containing MBCD. (A) After incubation, cells were fixed and analyzed by IF (magnification, ×10). T-Ag-positive cells were counted as BKV-infected cells, and the percentage was calculated against total cells. In the experiments whose results are

chloride (CsCl)-purified and Alexa Fluor 488-labeled BKV with Cav-1 or clathrin. Altogether, our data suggest that caveolar endocytosis is critical for BKV infection of HRPTEC.

MATERIALS AND METHODS

HRPTEC culture. HRPTEC, purchased from Cambrex Bio Science, Inc. (Walkersville, MD), were cultured as recommended by the manufacturer. Briefly, HRPTEC were plated for culture in renal epithelial cell basal medium (REBM) (Cambrex Bio Science, Inc.) containing 10% fetal bovine serum (FBS), renal epithelial cell growth medium (REGM) Single Quots (human epidermal growth factor, insulin, hydrocortisone, gentamicin/amphotericin-B (GA)-1000, epinephrine, triiodothyronine, transferrin) (Cambrex Bio Science, Inc.), and 100 units/ml penicillin-G (Invitrogen, Carlsbad, CA) in a humidified 5% CO_2 incubator at 37°C.

Viruses (propagation, purification, labeling, and titer). BKV was purchased from ATCC (Manassas, VA) and was propagated by the standard method described by Liu and Atwood (23). Briefly, HRPTEC were infected with BKV for 4 weeks, with the medium being changed and collected each week. After 4 weeks, the cells were harvested by scraping. All collected medium and harvested cells were centrifuged at 10,000 rpm for 15 min. Pellets were resuspended in 1/10 of the supernatant and then frozen at −80°C and thawed at 37°C three times. To release virus from the nucleus and cytoplasm, the cells were sonicated. Then, deoxycholate (Sigma-Aldrich, St. Louis, MO) was added at a final concentration of 0.25%, and the cells were incubated at 37°C for 30 min. The lysate and medium mixtures were centrifuged at 10,000 rpm for 30 min. The supernatant was saved for experimental use.

Virus containing supernatant was gently layered at the top of 20% sucrose and centrifuged at 100,000 × *g*, at 4°C, for 2 h in a 70 Ti rotor (Beckman, CA). The pellets were dissolved with buffer A (1 M Tris [pH 8], 5 M NaCl, 0.1 M $CaCl_2$) and sonicated for 30 s three times. The sonicated viral sample was overlaid on a CsCl density gradient (1.40 and 1.20 g/ml) and ultracentrifuged at 120,000 × *g* overnight. The viral fraction was extracted, diluted with buffer A, and again ultracentrifuged on the CsCl gradient. The viral fraction was extracted and dialyzed against buffer A at 4°C overnight. The purified virus was labeled by using an Alexa Fluor 488 microscale protein labeling kit (Molecular Probes, Eugene, OR) according to the manufacturer's instructions. Briefly, 100 μl of purified viral solution was transferred to a reaction tube and 10 μl of 1 M sodium bicarbonate was added.

Then, 33 nmol Alexa Fluor tetrafluorophenyl ester was added to the reaction tube and the mixture was incubated for 15 min. After the incubation, 50 μl of the conjugate reaction mixture was layered on the resin bed in the microcentrifuge tube and centrifuged at 16,000 × *g* for 1 min.

The viral titers were calculated in fluorescence-forming units (FFU) per ml by using the fluorescent focus assay described by Low et al. (24). This method is a variation of the plaque assay, to detect infected cells by indirect immunofluorescence analysis of T-Ag, detected with anti-SV40 T antigen mouse monoclonal antibody. Briefly, 70% confluent HRPTEC in 24-well plates were incubated with 10-fold serial dilutions of BKV for 72 h at 37°C. Fresh medium was then added, and the cells were incubated for another 48 h. The cells were fixed and analyzed by an immunofluorescence (IF) method. Infected cells were counted in five random areas of each coverslip, and the means ± standard deviations (SD) of the results were calculated from three different coverslips with the same amount of BKV.

Antibodies and agents. To detect T-Ag, anti-SV40 T antigen (Ab-2) mouse monoclonal antibody (PAb 418) was purchased from Calbiochem (San Diego, CA). These antibodies cross-react with the BKV T antigen. To detect Cav-1 and clathrin heavy chain (HC), Cav-1 rabbit polyclonal antibody and clathrin HC rabbit polyclonal antibody were purchased from Santa Cruz Biotechnology (Santa Cruz, CA). Glyceraldehyde-3-phosphate dehydrogenase (GAPDH) (Abcam, Cambridge, MA) was used as the loading control. For IF and Western blot (WB) analyses using an Odyssey system (LI-COR, Inc., Lincoln, NE), Alexa Fluor 488 goat anti-mouse immunoglobulin G (IgG) heavy plus light chains (H+L), Alexa Fluor 680 goat anti-mouse IgG (H+L), Alexa Fluor 680 goat anti-rabbit IgG (H+L) (Molecular Probes, Eugene, OR), and IRDye 800-conjugated, affinity-purified anti-rabbit IgG (H&L) (Rockland Immunochemicals, Inc., Gilbertsville, PA) were purchased. MBCD and Nys were purchased from Sigma-Aldrich and Calbiochem, respectively.

Infection and treatment. HRPTEC which had been passaged six to eight times were infected with BKV at a multiplicity of infection (MOI) of 0.5 FFU/cell at 37°C for 72 h. Fresh medium was added, and then the cells were incubated for another 48 h. The incubation with BKV after siRNA transfection was started 2 days after siRNA transfection. In the experiments using pharmacological agents, HRPTEC were preincubated with each agent at 37°C for 1 h. BKV was then added, and the mixture was coincubated for another 72 h at 37°C. After 72 h of coincubation, the cells were washed and incubated for another 48 h in medium containing each agent. HRPTEC not incubated with BKV and agents were used as a negative control.

Cytotoxicity assay. To investigate the cytotoxicities of MBCD and Nys, a CytoTox 96 nonradioactive cytotoxicity assay (Promega, Madison, WI) was used to measure the levels of lactate dehydrogenase (LDH) released, according to the manufacturer's manual and the method described by Allen and Rushton (2). Briefly, HRPTEC seeded on a 96-well plate were incubated with several doses of MBCD (1.25, 2.5, 5, and 10 mM) or Nys (12.5, 25, 50, 100, and 200 μg/ml) for 5 days. After the incubation, 50 μl of the supernatants and cell lysates from each well was transferred to a 96-well enzymatic assay plate and 50 μl of LDH colorimetric determination solution was added. The plates were incubated at room temperature, protected from light, for 30 min. Then, 50 μl of stop solution (1 M acetic acid) was added to each well and the level of LDH released was measured using the 96-well-plate reader.

siRNA. HRPTEC were grown to 60 to 80% confluence on a 60-mm dish and transfected with siRNA which targeted either the caveolin-1 or clathrin HC gene (Santa Cruz Biotechnology). Cells were transfected with 50 to 300 nM of caveolin-1 or clathrin HC siRNA containing 6 μl siRNA transfection reagent (Santa Cruz Biotechnology). After 48 h, the cells were used for the experiments.

WB analysis. After incubation with BKV and/or inhibitors, cell monolayers were washed three times with phosphate-buffered saline (PBS). Cells were scraped and harvested, and these samples were separated by sodium dodecyl sulfate-polyacrylamide gel electrophoresis using 10% Tris-HCl gel (Bio-Rad Laboratories, Hercules, CA). The gel-separated protein bands were blotted onto polyvinylidene difluoride membranes (Millipore Corporation, Bedford, MA). The membranes were blocked in Odyssey blocking buffer (LI-COR, Inc.) at room temperature for 1 h. After being blocked, the membranes were incubated with the first antibody (PAb 418, Cav-1, or GAPDH) at 4°C overnight with constant rotation. The membranes were then washed four times with Tris-buffered saline containing 0.1% Tween 20 (TTBS) at room temperature for 5 min with agitation and incubated with the secondary antibody (Alexa Fluor 680 or IRDye 800). The membranes were washed four times with TTBS at room temperature for 5 min with agitation. The bands were visualized by using an Odyssey infrared imaging system.

The integrated intensity of each signal was measured by using the Odyssey system, and the relative intensities of T-Ag and Cav-1 corrected by the intensity of GAPDH were expressed as graph bars.

Indirect IF analysis. HRPTEC seeded on coverslips were fixed in 100% methanol at −20°C for 20 min after three washes with PBS. After incubation in TTBS containing 3% bovine serum albumin for 30 min, the cells were incubated with the first antibody (1 μg/ml PAb 418 or a 1:50 dilution of Cav-1 or clathrin) diluted with TTBS containing 1% bovine serum albumin for 1 h and washed three times with TTBS for 5 min each. Then, the cells were incubated with the

shown in Fig. 3 and 4, untreated HRPTEC and HRPTEC incubated with BKV only were used as negative and positive controls. At least 500 cells were counted from three independent coverslips, and means and SE were calculated from the results of two independent experiments. *, $P < 0.02$; **, $P < 0.01$; ***, $P < 0.005$. (B) After incubation, cells were harvested and analyzed by WB. Relative levels of T-Ag expression were detected by using an Odyssey system to measure the intensities and depicted as graph bars. The intensity of T-Ag expression was corrected by the intensity of GAPDH as the loading control. Means and SE were calculated from the results of two independent experiments. Control, HRPTEC were not incubated with either BKV or MBCD; *, $P < 0.05$. (C) HRPTEC were preincubated with 5 mM of MBCD for 1 h prior to an 8-h coincubation with labeled BKV (MOI, 5 FFU/cell) and transferrin, (10.0 μg/ml). After cells were fixed, Alexa Fluor 488-labeled BKV (green) and Alexa Fluor 633-conjugated transferrin (red) were observed by confocal microscope using a 63× lens objective.

secondary antibody (a 1:200 dilution of Alexa Fluor 488 or 680) for 40 min and washed three times with TTBS for 5 min each.

To investigate the percentage of infected cells, a fluorescent microscope (Nikon Eclipse E600) was used to observe the cells, and SPOT version 4.0.9 (Diagnostic Instruments, Scotland, United Kingdom) was used to capture images. The percentage of infected cells was calculated by using the following formula: percentage of infected cells = number of T-Ag-positive cells/total number of cells × 100. To check that MBCD and Nys did not interfere with the clathrin-mediated pathway, we used transferrin from human serum conjugated to Alexa Fluor 633 (Molecular Probes). After 1 h of preincubation with MBCD or Nys, HRPTEC were coincubated with labeled BKV (5 FFU/cell) and transferrin (10.0 μg/ml) in medium containing MBCD (5 mM) or Nys (100 μg/ml) for 8 h. The cells were washed three times with PBS, fixed in 100% methanol at −20°C for 20 min, and then observed by using a confocal microscope (Leica TCS SP5), and images were captured by using the Leica application suite for advanced fluorescence.

To investigate the colocalization of labeled BKV with Cav-1 or clathrin, HRPTEC were incubated with labeled BKV at an MOI of 5 FFU/cell for 0 to 8 h at 37°C. A confocal microscope (Leica TCS SP5) was used to observe the cells, and the Leica application suite for advanced fluorescence was used to capture images. The colocalization area and viral-particle area were recognized by using a MetaVue imaging system (Molecular Devices Corporation, Sunnyvale, CA), and the colocalization rate was calculated by using the following formula: colocalization rate = area of viral particles colocalized with Cav-1/area of total viral particles × 100.

Statistical analysis. All experiments were repeated at least twice. The means ± SE were calculated from repeated data. Three-way analysis of variance (dose by BKV by replication) with Waller-Duncan correction for multiple comparisons was used for the WB analysis. Two-way analysis of variance with a linear contrast test for trend with dose with the Waller-Duncan multiple-comparison correction was used for the IF analysis. Three-way analysis of variance with a square root transform to stabilize the variance with the Waller-Duncan multiple-comparison adjustment was used for the colocalization study of labeled BKV with Cav-1 or clathrin. A global test of differences between Cav-1 and clathrin was performed before any comparisons were made.

RESULTS

Efficiency of BKV infection of HRPTEC in vitro. To optimize BKV infection protocols for HRPTEC, cells were incubated with BKV at MOIs from 0.5 to 5 FFU/cell and for time periods ranging from 1 h to 96 h. MOIs over 1.5 FFU/cell caused HRPTEC to detach from tissue-culture vessels within 4 h of incubation. When MOIs from 0.75 to 1 FFU/cell were used, HRPTEC still detached from the substrate at between 72 h and 96 h of incubation. Therefore, these results were not included in the data presented in Fig. 1. The percentage of infected cells gradually increased throughout the time course, but was not found to be dose dependent, due to the inability to test these higher MOIs. The highest percentage of infected cells was 36.4% ± 1.8% at an MOI of 0.5 FFU/cell and at 72 h of incubation (Fig. 1). This was the maximum infection possible in the absence of cell detachment and lysis.

Effect of cholesterol depletion on BKV infection. Caveolae are rich in several lipids, such as cholesterol, sphingolipids, ceramide, and ganglioside (36). Cholesterol is a principal structural lipid of caveolae. If caveolae play a pivotal role for BKV entry into HRPTEC, the depletion of plasma membrane cholesterol would interfere with BKV infection. To evaluate the role of caveolae in BKV infection, we used MBCD and Nys as cholesterol-depleting agents (17).

Appropriate concentrations of MBCD and Nys were determined by measuring released LDH as a marker of cytotoxicity. When HRPTEC were incubated with MBCD at 1.25, 2.5, 5, and 10 mM, there was no significant difference between the levels of LDH release in comparison to the level in the control (nontreated cells) (Fig. 2A). Likewise, Nys at 12.5, 25, 50, and 100 μg/ml did not affect LDH release, but 200 μg/ml Nys caused a significant increase of LDH release ($P < 0.05$) (Fig. 2B). These results indicated that concentrations of MBCD below 10 mM and concentrations of Nys up to 100 μg/ml had no significant cytotoxic effect. Therefore, we used 1.25, 2.5, and 5 mM MBCD and 12.5, 25, 50, and 100 μg/ml Nys in our experiments.

In the results of the IF analysis, the percentage of BKV-infected cells was 32.55% ± 1.09% when HRPTEC were incubated with BKV alone. The percentage of infected cells declined substantially when cells were incubated with BKV and increasing doses of MBCD (1.25 mM, $P < 0.02$; 2.5 mM, $P < 0.01$; and 5 mM, $P < 0.005$), and the trend was significant ($P < 0.005$) (Fig. 3A). There were no T-Ag-positive cells when HRPTEC were incubated with either MBCD only or BKV only (Fig. 3A). As expected, WB analysis did not detect any T-Ag signal in the control groups (untreated HRPTEC and HRPTEC incubated with MBCD alone). However, when HRPTEC were incubated with BKV, the T-Ag signal was prominent and significantly exceeded the T-Ag signals in HRPTEC coincubated with BKV and various doses of MBCD. The relative level of T-Ag expression in HRPTEC coincubated with BKV and the highest dose of MBCD (5 mM) was significantly lower than the signal in cells incubated with BKV alone ($P < 0.05$). There was also a significant decreasing trend with dose in HRPTEC incubated with BKV versus cells coincubated with BKV and various doses of MBCD ($P < 0.01$) (Fig. 3B). Almost all of the Alexa Fluor 633-conjugated transferrin, a marker of clathrin-mediated endocytosis, was located in the cytoplasm at 8 h after incubation in MBCD-containing medium, whereas almost all of the Alexa Fluor 488-labeled BKV particles were unable to enter the cytoplasm and were located on the cell surface (Fig. 3C).

The percentages of BKV-infected cells in HRPTEC coincubated with BKV and several doses of Nys (12.5, 25, 50, and 100 μg/ml) were significantly decreased ($P < 0.01$, $P < 0.005$, $P < 0.005$, and $P < 0.002$, respectively) compared to the percentage of infected cells in HRPTEC incubated with BKV alone, and the trend was significant ($P < 0.004$) in the evaluation using IF testing (Fig. 4A). In the WB analysis results, the relative T-Ag expression levels were also significantly lower ($P < 0.001$) when HRPTEC were coincubated with BKV and several doses of Nys than in HRPTEC incubated with BKV alone, and there was also a significant decreasing trend with dose in HRPTEC incubated with BKV versus cells coincubated with BKV and various doses of Nys ($P < 0.01$) (Fig. 4B). Alexa Fluor 633-conjugated transferrin was located in the cytoplasm at 8 h after incubation in Nys-containing medium, whereas Alexa Fluor 488-labeled BKV particles were unable to enter the cytoplasm and were mainly located on the cell surface (Fig. 4C).

Thus, these results demonstrate that cholesterol depletion causes inhibition of BKV infection of HRPTEC without interference with the clathrin-mediated pathway of endocytosis.

Effect of siRNA-mediated Cav-1 knockout on BKV infection. Caveolin-1 (Cav-1) is an integral membrane protein and a main component of caveolae. Disruption of Cav-1 prevents caveola-mediated internalization. We introduced Cav-1 siRNA into HRPTEC to evaluate the role of Cav-1 in BKV infection and used clathrin siRNA as the control. Clathrin protein is the

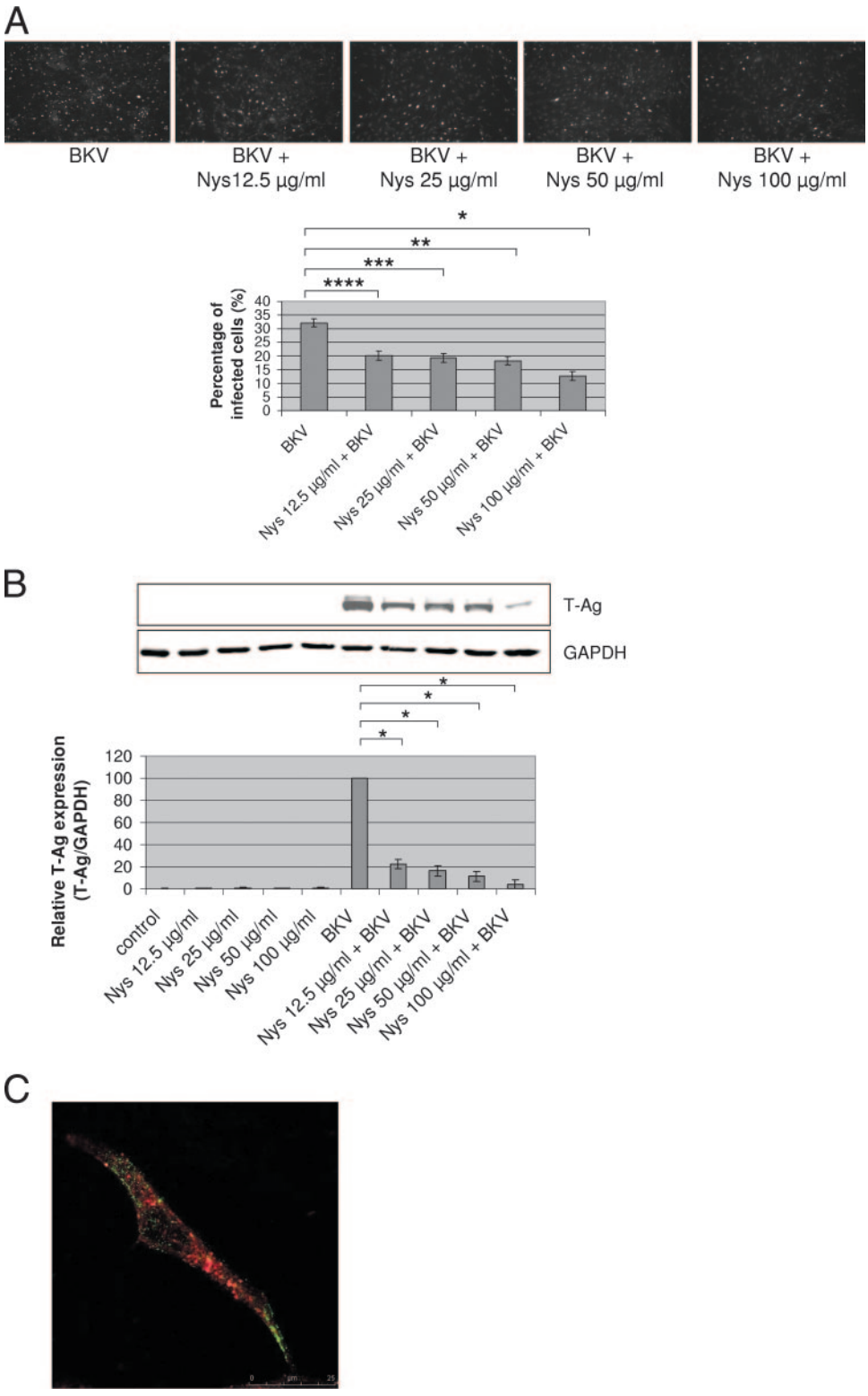

FIG. 4. Nys interfered with BKV infection. HRPTEC were preincubated with Nys (12.5, 25, 50, and 100 µg/ml) for 1 h prior to coincubation with BKV (MOI, 0.5 FFU/cell) and Nys for 72 h. The medium was removed, and cells were washed three times with REBM with 0.5% FBS and incubated for another 48 h with fresh medium containing Nys. (A) After incubation, cells were fixed and analyzed by IF (magnification, ×10). T-Ag-positive cells were counted as BKV-infected cells, and the percentage was calculated against total cells. At least 500 cells were counted from three independent coverslips, and means and SE were calculated from two independent experiments. *, $P < 0.01$; **, $P < 0.005$; ***, $P < 0.005$; ****, $P < 0.002$. (B) After incubation, cells were harvested and analyzed by WB. Relative levels of T-Ag expression were detected by measuring the intensities with an Odyssey system and depicted as graph bars. The intensity of T-Ag expression was corrected by the intensity of GAPDH as the loading control. Means and SE were calculated from the results of two independent experiments. Control, HRPTEC were not incubated with either BKV or Nys; *, $P < 0.001$. (C) HRPTEC were preincubated with 100 µg/ml of Nys for 1 h prior to 8 h of coincubation with labeled BKV (MOI, 5 FFU/cell) and transferrin (10.0 µg/ml). After cells were fixed, Alexa Fluor 488-labeled BKV (green) and Alexa Fluor 633-conjugated transferrin (red) were observed by confocal microscope using a 63× lens objective.

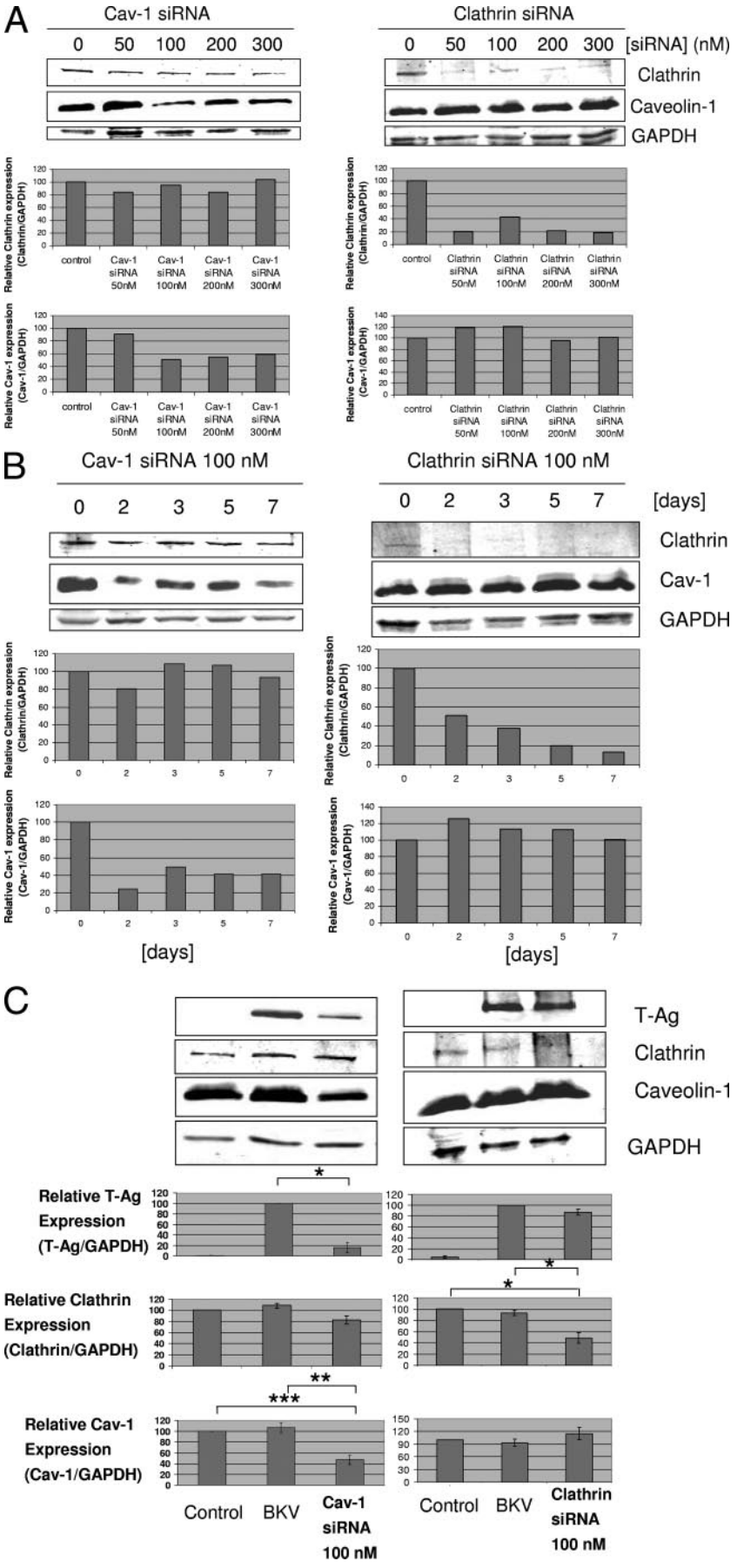
A
Cav-1 siRNA
0 50 100 200 300
Clathrin siRNA
0 50 100 200 300 [siRNA] (nM)
Clathrin
Caveolin-1
GAPDH
Relative Clathrin expression (Clathrin/GAPDH)
Relative Cav-1 expression (Cav-1/GAPDH)
control
Cav-1 siRNA 50nM
Cav-1 siRNA 100nM
Cav-1 siRNA 200nM
Cav-1 siRNA 300nM
Clathrin siRNA 50nM
Clathrin siRNA 100nM
Clathrin siRNA 200nM
Clathrin siRNA 300nM
B
Cav-1 siRNA 100 nM
Clathrin siRNA 100 nM
0 2 3 5 7
[days]
Clathrin
Cav-1
GAPDH
C
T-Ag
Clathrin
Caveolin-1
GAPDH
Relative T-Ag Expression (T-Ag/GAPDH)
Relative Clathrin Expression (Clathrin/GAPDH)
Relative Cav-1 Expression (Cav-1/GAPDH)
Control
BKV
Cav-1 siRNA 100 nM
Clathrin siRNA 100 nM

major constituent of the clathrin-coated pits and coated vesicles formed during clathrin-mediated endocytosis. Clathrin-mediated endocytosis is an alternative to the caveolar endocytosis pathway for the uptake of extracellular material into the cell. As to polyomavirus, JCV was reported to enter into cells through clathrin-mediated endocytosis (32).

At the outset, we calculated an appropriate effective dose of Cav-1 and clathrin siRNAs for transfection and also confirmed that the effect of siRNA is still present at least 7 days after transfection with siRNA (required period of incubation with BKV after siRNA transfection). Figure 5A shows that, when 100 nM or greater of Cav-1 siRNA was used to transfect cells, the relative Cav-1 expression level was dramatically lower than the level in untransfected cells, while the clathrin expression level was not affected by Cav-1 siRNA transfection. The clathrin expression level when clathrin siRNA was used to transfect cells was also dramatically lower than in untransfected cells, whereas the Cav-1 expression level was not affected by clathrin siRNA transfection. As shown in Fig. 5B, the levels of Cav-1 and clathrin expression were low for 7 days after siRNA transfection.

We incubated HRPTEC with BKV 2 days after transfection with 100 nM of Cav-1 or clathrin siRNA (Fig. 5C). At 7 days after siRNA transfection (at 5 days after incubation with BKV), the relative level of Cav-1 expression in HRPTEC incubated with BKV and transfected with 100 nM Cav-1 siRNA was significantly lower than the levels in control HRPTEC ($P < 0.03$) and HRPTEC incubated with BKV without siRNA transfection ($P < 0.05$). There was no significant difference between control HRPTEC and HRPTEC incubated with BKV without siRNA transfection with regard to the Cav-1 expression level. Correspondingly, the relative T-Ag expression level when HRPTEC were incubated with BKV and transfected with 100 nM Cav-1 siRNA was also significantly lower than the level in HRPTEC incubated with BKV without siRNA transfection ($P < 0.01$). There was no effect of Cav-1 siRNA transfection upon clathrin expression.

On the contrary, after clathrin siRNA transfection, the relative level of T-Ag expression was not different between HRPTEC incubated with BKV with or without transfection with 100 nM clathrin siRNA, though the level of clathrin expression of HRPTEC incubated with BKV with clathrin siRNA transfection was significantly lower than in the control HRPTEC ($P < 0.01$) and HRPTEC incubated with BKV without clathrin siRNA transfection ($P < 0.01$).

These results indicated that knocking down Cav-1 by means of siRNA interfered with BKV infection of HRPTEC, whereas knocking down clathrin did not.

Colocalization of BKV with caveolin-1 or clathrin. Figure 6A shows colocalization with Cav-1 or clathrin of Alexa Fluor 488-labeled BKV after CsCl purification. HRPTEC were incubated with labeled BKV for 0 to 8 h at an MOI of 5 FFU/cell. At 0 and 1 h, BKV particles were not detected in HRPTEC (0-h pictures are not shown). At 2 h, several BKV particles were located on the cell surface, but few BKV particles were colocalized with Cav-1. BKV particles which were located on the cell surface and colocalized with Cav-1 were more numerous at 4 h. At 6 and 8 h, BKV particles were located not only on the cell surface, but also in the cytoplasm. On the other hand, the rate of colocalization of labeled BKV particles with clathrin at 4 h was insignificant and was much less than the colocalization with Cav-1. Figure 6B shows the results of quantitative analysis of the colocalization rate of labeled BKV with Cav-1 or clathrin. The colocalization rate of BKV with Cav-1 increased gradually, peaked at 4 h, and decreased gradually after a 4-h incubation period. The colocalization rate at 4 h was significantly higher than at 2 h ($P < 0.005$) and 6 h ($P < 0.01$). On the contrary, labeled BKV particles were hardly colocalized with clathrin through the entire incubation period, and the colocalization rate of BKV with Cav-1 at each time point was significantly higher than with clathrin (4 h, $P < 0.001$; 6 h, $P < 0.05$; 8 h, $P < 0.05$). Figure 6C shows the results of image cross-correlation spectroscopy (39). Both upper panels show labeled BKV, with Cav-1 (left) and clathrin (right) at 4 h after infection. The graphs show that the cross-correlation of labeled BKV with Cav-1 was much higher than with clathrin at 4 h after infection.

These results indicated that BKV started to be attached on the cell surface within 2 h after incubation, remained trapped in the caveolae about 4 h after infection, and then entered into HRPTEC through the caveolae after 6 h, and BKV internalization did not depend on the clathrin endocytic pathway.

DISCUSSION

BKV nephritis has become a severe problem for renal transplant patients, with about half of the cases of BKV nephritis becoming graft losses. However, there are few in vitro studies of BKV infection and only three reports of in vitro BKV infection of HRPTEC (1, 25, 24). It seems that the nature of the host cells has a profound effect upon the efficiency and consequences of viral infection. Therefore, it is imperative to

FIG. 5. Cav-1 siRNA decreased BKV infection of HRPTEC, whereas clathrin siRNA was ineffective. Levels of Cav-1 and clathrin expression were analyzed by WB. Relative T-Ag, Cav-1, and clathrin expression levels were calculated as the ratio between the intensities of the T-Ag, Cav-1, or clathrin bands and the GAPDH band (equal loading control) measured by using the Odyssey system, and the results were presented as graph bars. Means and SE were calculated from the results of at least two independent experiments. *, $P < 0.01$; **, $P < 0.03$; ***, $P < 0.05$. (A) Dose dependence of siRNA transfection. HRPTEC were transfected with 50 to 300 nM of either Cav-1 siRNA or clathrin siRNA. At 48 h after transfection, cells were harvested and analyzed by WB. (B) Time course of 100 nM and 200 nM Cav-1 siRNA transfection. HRPTEC were transfected with 100 nM Cav-1 and clathrin siRNA. Cells were harvested at 2, 3, 5, and 7 days after transfection and analyzed by WB. (C) Cav-1 siRNA transfection interfered with BKV infection. HRPTEC were transfected with 100 nM either of Cav-1 or clathrin siRNA. HRPTEC were incubated with BKV at 2 days after administration of Cav-1 or clathrin siRNA, fresh medium was added 5 days after siRNA transfection, and cells were harvested 7 days after transfection. Control, HRPTEC neither incubated with BKV nor transfected with siRNA. BKV, HRPTEC incubated with BKV but not transfected with siRNA.

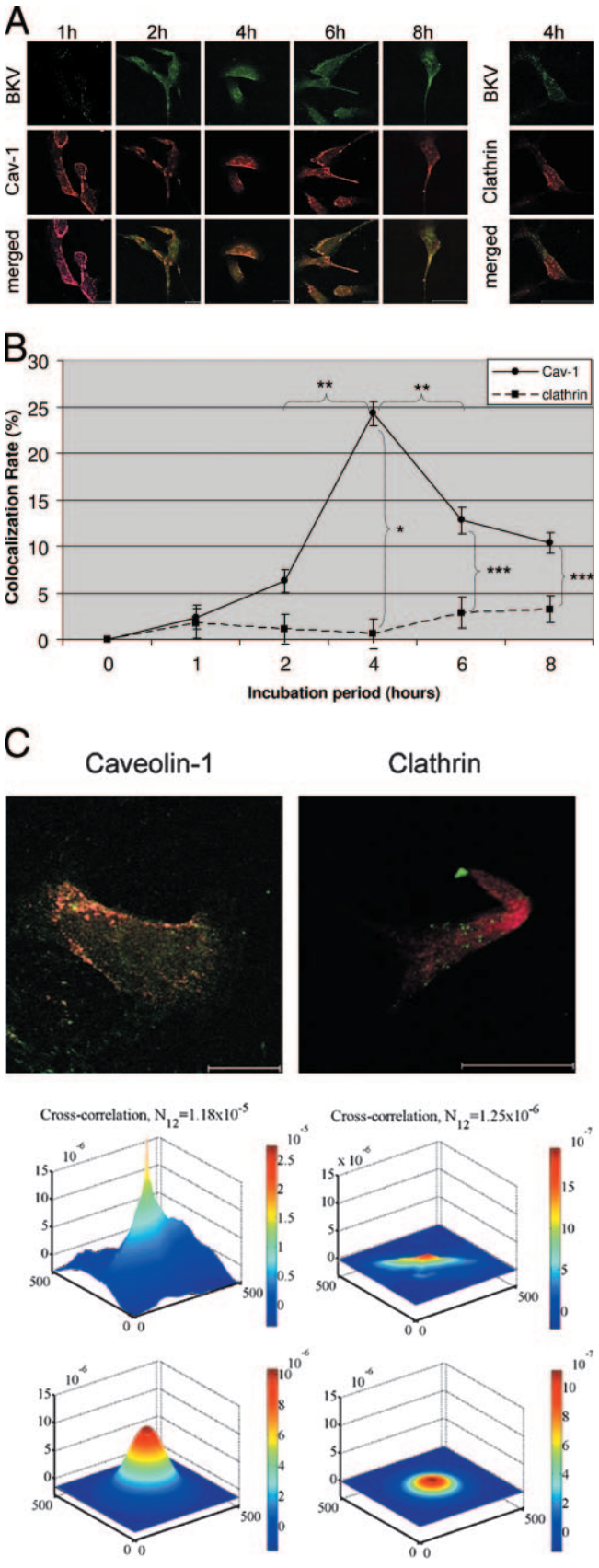

FIG. 6. Colocalization of labeled BKV with Cav-1 or clathrin. (A) Colocalization of BKV with Cav-1 or clathrin. HRPTEC were incubated with Alexa Fluor 488-labeled BKV (green) for 0 to 8 h. After incubation, cells were fixed, immunofluoresced for anti-Cav-1 antibody (red) or anti-clathrin antibody (red), and analyzed by confocal microscope using a 63× lens objective. Bars represent 25 μm. Labeled BKV particles colocalized with Cav-1 or clathrin were expressed as yellow pixels in merged image. (B) Time course and quantitative analysis of colocalization. Colocalization rates of labeled BKV with Cav-1 and clathrin were calculated from the results for at least 100 cells randomly selected from three independent experiments and evaluated from each incubation period. The colocalization threshold and viral particle threshold were determined automatically and regularly by finding the higher intensity value for yellow pixels and green pixels. Means and SE were calculated from the results of at least two independent experiments. *, $P < 0.001$; **, $P < 0.01$; ***, $P < 0.05$. (C) Image cross-correlation analysis. Colocalization of viral particles (Alexa Fluor 488, green) with their potential fusion protein partner of endocytosis, caveolin or clathrin (Alexa Fluor 680, red), was analyzed. The peak height of cross correlation data indicating the degree of cross-correlation in green pixels with the red pixels of caveolin (upper left graph) was much higher than that of clathrin (upper right graph). Fitting the raw data with an analytical correlation function allowed the quantitative estimation of the degree of cross correlation (N_{12}) (lower left graph for caveolin and lower right graph for clathrin). Overlap of excitation signal between the two dyes was negligible.

use HRPTEC, one of the main natural targets of BKV infection, in order to elucidate the exact mechanism of BKV nephritis in humans. Low et al. reported that BKV actually infected HRPTEC in vitro, as detected by the expression of high levels of T-Ag, VP1, and viral DNA 36 h after infection (24). The role of caveolae in BKV internalization in human cells was not addressed in detail.

Though it is still controversial whether caveolae play a role in endocytosis, SV40 has been reported to internalize through caveolae (4, 5, 15, 24, 26, 28–31, 33, 35) and BKV has also been reported to internalize into HRPTEC through flask-like invaginations similar to caveolae, as shown by morphological analysis (8). Moreover, previous reports indicated that N-linked glycoprotein with α(2,3)-linked sialic acid served as a BKV receptor in monkey-derived Vero cells (9, 10), and gangliosides GD1b and GT1b were also reported to work as receptors for BKV in human prostate carcinoma cells (25). Since these gangliosides seem to be strongly associated with caveolae, it is possible that caveolae also play a role in endocytosis for BKV.

At first, we focused on establishing an experimental protocol for incubating HRPTEC with BKV. Low et al. reported that high levels of T-Ag were expressed at 36 h when HRPTEC were infected with BKV at an MOI of 5 FFU/cell (24). Our results showed the highest percentage of BKV infection at 72 h when HRPTEC were infected with BKV at an MOI of 0.5 FFU/cell. As this MOI was lower than that utilized by Low et al., the apparent infection timing may have been longer than what was reported previously (24).

We then examined the role of cholesterol in BKV internalization by using the cholesterol-depleting agents MBCD and Nys. Our results suggested that cholesterol was required for BKV infection of HRPTEC, because MBCD or Nys caused inhibition of BKV infection in HRPTEC and they did not interfere with the internalization of transferrin, which is a marker of clathrin endocytosis. These results indicated that

BKV entered HRPTEC through structures in the cell membrane that are enriched in cholesterol, such as caveolae, and these agents had no effect upon the clathrin-mediated pathway. Damm et al. (5) and Pelkmans et al. (31) reported that a combination of Nys and progesterone blocked SV40 infection of a human hepatoma cell line (HuH7 cells) and CV-1 cells. Gilbert et al. reported that MBCD or Nys inhibited SV40 infection of murine fibroblasts (NIH 3T3 cells) and primary baby mouse kidney epithelial cells, and also reported that MBCD or Nys inhibited mPy infection against GD1a-supplemented rat glioma cells (C6 cells) (16). These results implied that SV40 and mPy entered cells through the caveolae. Moreover, BKV infection of monkey-derived Vero cells was reported to be inhibited by MBCD (12), providing additional support for our conclusion. Thus, our experiments strongly support a role for cholesterol in BKV internalization into cells.

Caveolins are scaffolding domains of caveolae. Three caveolins exist: caveolin-1, caveolin-2, and caveolin-3. Caveolin-1 and -2 are coexpressed in most cells; caveolin-3 is expressed in muscle-specific cells, such as skeletal, cardiac, and smooth muscle cells. Caveolin-1 expression can induce the formation of caveolae, but caveolin-2 cannot. Therefore, disruption of the caveolin-1 gene results in the abolishment of caveolae (22, 34, 36). Our results showed that siRNA-mediated Cav-1 knockout caused inhibition of BKV infection in HRPTEC, but clathrin knockout did not. It seems likely that BKV enters HRPTEC through caveolae and not through the clathrin-mediated pathway. Eash et al. reported that BKV infection of Vero cells was inhibited by the expression of a dominant-negative Cav-1 mutant compared to the infection of Vero cells expressing wild-type Cav-1. Despite the different host cells, our data are in good concordance with their results (12). We also investigated the dynamics of the colocalization of labeled BKV with Cav-1. Labeled BKV particles were colocalized with Cav-1, but not with clathrin, and the colocalization rate of labeled BKV with Cav-1 peaked at 4 h after incubation. Our data suggest that BKV entered HRPTEC through caveolae and that, at about 4 h after infection, BKV particles were mostly trapped in the caveolae. Pelkmans et al. (30) and Gilbert and Benjamin (15) reported colocalization of polyomaviruses SV40 and mPy with Cav-1. These viruses were frequently trapped in caveolae until 1 h after incubation. Our data suggest that the internalization of BKV proceeds relatively slowly.

To understand more precisely the mechanisms and kinetics of BKV infection, it is important to employ HRPTEC, which are the main target of BKV infection in the actual clinical situation. It must be taken into consideration that the viral life cycles are quite different in each cell type. For example, SV40 was reported to be unable to infect HRPTEC (24), but was efficient in the infection of monkey tubular epithelial cells (16), HuH7 cells (5), NIH 3T3 cells (16), and CV-1 cells (30, 31, 35). mPy was reported not to enter NIH 3T3 cells and baby mouse kidney epithelial cells via caveolae (16), in contrast to normal murine mammary gland epithelial cells (35). These differences seem to come from the inherent specificities of the polyomaviruses for each of the different cell lines.

In summary, our results show that depletion of cholesterol and disruption of Cav-1 mRNA inhibit BKV infection of HRPTEC, and labeled BKV particles were colocalized with Cav-1. Considering that Cav-1 is a scaffolding protein of caveolae and cholesterol is abundant in caveolae, our results suggest that BKV enters HRPTEC through caveolae in vitro. Moreover, our results indicate that BKV are trapped in caveolae most frequently at 4 h after infection. BKV infection is relatively slow in comparison to mPy and SV40 infection.

ACKNOWLEDGMENTS

We thank Raymond Hoffmann (Medical College of Wisconsin [MCW]) for help with statistical analysis and Simon Prosser (MCW), Rimas Orentas (MCW), and Sundaram Hariharan (MCW) for critical reading of the manuscript.

This work was supported by a program development grant from the Department of Medicine, Medical College of Wisconsin (A.S.) and NIH grant R01 HL022563 (A.S.).

REFERENCES

1. **Abend, J. R., J. A. Low, and M. J. Imperiale.** 2006. Inhibitory effect of gamma interferon on BK virus gene expression and replication. J. Virol. **81:**272–279.
2. **Allen, M. J., and N. Rushton.** 1994. Use of the CytoTox 96 assay in routine biocompatibility testing in vitro. Promega Notes **45:**7–10.
3. **Celik, B., and P. S. Randhawa.** 2004. Glomerular change in BK virus nephropathy. Hum. Pathol. **35:**367–370.
4. **Chen, Y., and L. C. Norkin.** 1999. Extracellular simian virus 40 transmits a signal that promotes virus enclosure within caveolae. Exp. Cell Res. **246:**83–90.
5. **Damm, E. M., L. Pelkmans, J. Kartenbeck, A. Mezzacasa, T. Kurzchalia, and A. Helenius.** 2005. Clathrin- and caveolin-1-independent endocytosis: entry of simian virus 40 into cells devoid of caveolae. J. Cell Biol. **168:**477–488.
6. **Deurs, B. V., K. Roepstorff, A. M. Hommelgaard, and K. Sandvig.** 2003. Caveolae: anchored, multifunctional platforms in the lipid ocean. Trends Cell Biol. **13:**92–100.
7. **Drachenberg, C. B., H. H. Hirsch, E. Ramos, and J. C. Papadimitriou.** 2005. Polyomavirus disease in renal transplantation. Review of pathological findings and diagnostic methods. Hum. Pathol. **36:**1245–1255.
8. **Drachenberg, C. B., J. C. Papadimitriou, R. Wali, C. L. Cubitt, and E. Ramos.** 2003. BK polyoma virus allograft nephropathy: ultrastructural features from viral cell entry to lysis. Am. J. Transplant. **3:**1383–1392.
9. **Dugan, A. S., S. Eash, and W. J. Atwood.** 2005. An N-linked glycoprotein with $\alpha(2,3)$-linked sialic acid is a receptor for BK virus. J. Virol. **79:**14442–14445.
10. **Dugan, A. S., S. Eash, and W. J. Atwood.** 2006. Update on BK virus entry and intracellular trafficking. Transpl. Infect. Dis. **8:**62–67.
11. **Eash, S., and W. J. Atwood.** 2005. Involvement of cytoskeletal components in BK virus infectious entry. J. Virol. **79:**11734–11741.
12. **Eash, S., W. Querbes, and W. J. Atwood.** 2004. Infection of Vero cells by BK virus is dependent on caveolae. J. Virol. **78:**11583–11590.
13. **Fishman, J. A.** 2002. BK virus nephropathy—polyomavirus adding insult to injury. N. Engl. J. Med. **347:**527–530.
14. **Gardner, S. D., A. M. Field, D. V. Coleman, and B. Hulme.** 1971. New human papovavirus (B.K.) isolated from urine after renal transplantation. Lancet **i:**1253–1257.
15. **Gilbert, J., and T. Benjamin.** 2004. Uptake pathway of polyomavirus via ganglioside GD1a. J. Virol. **78:**12259–12267.
16. **Gilbert, J. M., I. G. Goldberg, and T. L. Benjamin.** 2003. Cell penetration and trafficking of polyomavirus. J. Virol. **77:**2615–2622.
17. **Goluszko, P., and B. Nowicki.** 2005. Membrane cholesterol: a crucial molecule affecting interactions of microbial pathogens with mammalian cells. Infect. Immun. **73:**7791–7796.
18. **Hariharan, S.** 2006. BK virus nephritis after renal transplantation. Kidney Int. **69:**655–662.
19. **Hirsch, H. H.** 2005. BK virus. Opportunity makes a pathogen. Clin. Infect. Dis. **41:**354–360.
20. **Hirsch, H. H., D. C. Brennan, C. B. Drachenberg, F. Ginevri, J. Gordon, A. P. Limaye, M. J. Mihatsch, V. Nickeleit, E. Ramos, P. Randhawa, R. Shapiro, J. Steiger, M. Suthanthiran, and J. Trofe.** 2005. Polyomavirus-associated nephropathy in renal transplantation: interdisciplinary analyses and recommendations. Transplantation **79:**1277–1286.
21. **Hirsch, H. H., and J. Steiger.** 2003. Polyomavirus BK. Lancet **3:**611–623.
22. **Kim, H. C., E. A. Hwang, M. J. Kang, S. Y. Han, S. B. Park, and K. K. Park.** 2004. BK virus infection in kidney transplant recipients. Transplant. Proc. **36:**2113–2115.
23. **Liu, C. K., and W. J. Atwood.** 2000. Propagation assay of the JC virus. Methods Mol. Biol. **165:**9–17.
24. **Low, J., H. D. Humes, M. Szczypka, and M. Imperiale.** 2004. BKV and SV40 infection of human kidney tubular epithelial cells in vitro. Virology **323:**182–188.
25. **Low, J. A., B. Magnuson, B. Tsai, and M. J. Imperiale.** 2006. Identification

of gangliosides GD1b and GT1b as receptors for BK virus. J. Virol. **80:**1361–1366.
26. **Nichols, B.** 2003. Caveosomes and endocytosis of lipid rafts. J. Cell Sci. **116:**4707–4714.
27. **Nickeleit, V., H. K. Singh, and M. J. Mihatsch.** 2003. Polyomavirus nephropathy: morphology, pathophysiology, and clinical management. Curr. Opin. Nephrol. Hypertens. **12:**599–605.
28. **Pelkmans, L., and A. Helenius.** 2002. Endocytosis via caveolae. Traffic **3:**311–320.
29. **Pelkmans, L., and A. Helenius.** 2003. Insider information: what viruses tell us about endocytosis. Curr. Opin. Cell Biol. **15:**414–422.
30. **Pelkmans, L., J. Kartenbeck, and A. Helenius.** 2001. Caveolae endocytosis of simian virus 40 reveals a new two step vesicular transport pathway to the ER. Nat. Cell Biol. **3:**473–483.
31. **Pelkmans, L., D. Pünterner, and A. Helenius.** 2002. Local actin polymerization and dynamin recruitment in SV40-induced internalization of caveolae. Science **296:**535–539.
32. **Pho, M. T., A. Ashok, and W. J. Atwood.** 2000. JC virus enters human glial cells by clathrin-dependent receptor-mediated endocytosis. J. Virol. **74:**2288–2292.
33. **Pietiäinen, V. M., V. Marjomäki, J. Heino, and T. Hyypiä.** 2005. Viral entry, lipid rafts and caveosomes. Ann. Med. **37:**394–403.
34. **Richards, A. A., and R. G. Parton.** 2003. Lipid rafts and caveolae as portals for endocytosis: new insights and common mechanisms. Traffic **4:**724–738.
35. **Richterová, Z, D. Liebl, M. Horák, Z. Palková, J. Štolrová, P. Hozák, and J. Forstová.** 2001. Caveolae are involved in the trafficking of mouse polyomavirus virions and artificial VP1 pseudocapsids toward cell nuclei. J. Virol. **75:**10880–10891.
36. **Smart, E. J., G. A. Graf, M. A. McNiven, W. C. Sessa, J. A. Engelman, P. E. Scherer, T. Okamoto, and M. P. Lisanti.** 1999. Caveolins, liquid-ordered domains, and signal transduction. Mol. Cell. Biol. **19:**7289–7304.
37. **Trofe, J., J. Gordon, P. Roy-Chaundhury, I. G. Koralnik, W. J. Atwood, R. R. Alloway, K. Khalilli, and E. S. Woodle.** 2004. Polyomavirus nephropathy on kidney transplantation. Prog. Transplant. **14:**130–140.
38. **Vasudev, B., S. Hariharan, S. A. Hussain, Y. R. Zhu, B. A. Bresnahan, and E. P. Cohen.** 2005. BK virus nephritis: risk factors, timing, and outcome in renal transplant patients. Kidney Int. **68:**1834–1839.
39. **Wiseman, P. W., C. M. Brown, D. J. Webb, B. Hebert, N. L. Johnson, J. A. Squier, M. H. Ellisman, and A. F. Horwitz.** 2004. Spatial mapping of integrin interactions and dynamics during cell migration by image correlation microscopy. J. Cell Sci. **117:**5521–5534.